Proceedings of ASME-JSME-KSME Joint Fluids Engineering Conference 2011
AJK2011-FED
July 24-29, 2011, Hamamatsu, Shizuoka, JAPAN

AJK2011-16027

THE EFFECT OF INNER SURFACE ROUGHNESS AND HEATING ON FRICTION FACTOR IN HORIZONTAL MICRO-TUBES

Lap Mou Tam
Department of Electromechanical Engineering, Faculty of Science and Technology, University of Macau, Av. Padre Tomás Pereira, Taipa, Macau, China.
Institute for the Development and Quality, Macau.

Hou Kuan Tam
Department of Electromechanical Engineering, Faculty of Science and Technology, University of Macau, Av. Padre Tomás Pereira, Taipa, Macau, China.

Afshin J. Ghajar
School of Mechanical and Aerospace Engineering, Oklahoma State University, Stillwater, Oklahoma, USA.

Wa San Ng
Department of Electromechanical Engineering, Faculty of Science and Technology, University of Macau, Av. Padre Tomás Pereira, Taipa, Macau, China.

Ieok Wa Wong
Department of Electromechanical Engineering, Faculty of Science and Technology, University of Macau, Av. Padre Tomás Pereira, Taipa, Macau, China.

Ka Fu Leong
Department of Electromechanical Engineering, Faculty of Science and Technology, University of Macau, Av. Padre Tomás Pereira, Taipa, Macau, China.

Choi Keng Wu
Department of Electromechanical Engineering, Faculty of Science and Technology, University of Macau, Av. Padre Tomás Pereira, Taipa, Macau, China.

ABSTRACT

According to Krishnamoorthy et al. [1], pressure drop measurements for horizontal micro-tubes under isothermal condition have been conducted by various researchers in recent years. From their literature review, it was shown that the friction factor in micro-tubes could unanimously be predicted by using macro-scale theory and that there is a need to investigate certain issues like (a) the effect of micro-tube diameter on the transition Reynolds number range and (b) the effect of the inner surface roughness on the friction factor and transition region. Regarding to the point (a), Ghajar et al. [2] measured the pressure drop for ~~a~~ horizontal mini- and micro-tubes with various diameters in the transition region under isothermal condition. Their experimental results indicated the influence of the tube diameter on the friction factor profile and on the transition Reynolds number range. However, regarding to the point (b), the effect of roughness on friction factor profile and transition was still not fully understood. Moreover, only a few studies have investigated the effect of heating on friction factor in micro-tubes, especially, in the transition region.

Therefore, in this study, an experimental setup was built to measure pressure drop for horizontal micro-tubes under the isothermal and uniform wall heat flux boundary conditions. Water was used as the test fluid and the test section was glass and stainless steel micro-tubes with various roughness and diameters. From the measurements, the effect of roughness and heating on friction factor and transition region was clearly observed. For friction factor under isothermal condition, compared to the macro-tube, the micro-tube had a narrower transition region due to the roughness and the decrease in the tube diameter delayed the start of transition. For friction factor under heating condition, the laminar and transition data were different from the isothermal case. Heating also delayed the start of transition. The effect of heating was not seen on the turbulent region. For isothermal and heating boundary conditions, the increase of inner surface roughness induced a narrower transition region.

Keywords: friction factor, inner surface roughness, micro-tube, transition

NOMENCLATURE

f fully developed friction factor coefficient (Darcy friction factor), ($=2 \cdot D \cdot \Delta P / \rho \cdot L \cdot V^2$), dimensionless
c_p specific heat of the test fluid evaluated at T_b, J/(kg·K)
D inside diameter of the test section (tube), m
h fully developed peripheral heat transfer coefficient, W/(m^2·K)
k thermal conductivity, W/(m^2·K) evaluated at T_b, W/(m·K)
L length of the test section (tube), m
Nu local average or fully developed peripheral Nusselt number ($= h \cdot D / k$), dimensionless
Pr local bulk Prandtl number ($=c_p \cdot \mu_b / k$), dimensionless
Ra surface roughness, μm
Re local bulk Reynolds number ($=\rho \cdot V \cdot D / \mu_b$), dimensionless
St local average or fully developed peripheral Stanton number [$=Nu / (Pr \cdot Re)$], dimensionless
T_b local bulk temperature of the test fluid, °C
T_w local inside wall temperature, °C
V average velocity in the test section, m/s
x local axial distance along the test section from the inlet, m

Greek Symbols
ΔP pressure difference, Pa
μ_b absolute viscosity of the test fluid evaluated at T_b, Pa·s
μ_w absolute viscosity of the test fluid evaluated at T_w, Pa·s
ρ density of the test fluid evaluated at T_b, kg/m^3
ε roughness height, m

INTRODUCTION

Due to rapid advancement in fabrication techniques, the miniaturization of devices and components is ever increasing in many applications. Whether it is in the application of miniature heat exchangers, fuel cells, pumps, compressors, turbines, sensors, or artificial blood vessels, a sound understanding of fluid flow in micro-scale channels and tubes is required. Indeed, within this last decade, countless researchers have been investigating the phenomenon of fluid flow in mini-, micro-, and even nanochannels. One major area of research in the phenomenon of fluid flow in mini- and microchannels is the friction factor. However, amidst all the investigations in mini- and microchannel flow, there seem to be a lack in the study of the flow in the transition region. One obvious question is the location of the transition region with respect to the hydraulic diameter of the channel and the roughness of the channel. To successfully understand friction factor and the location of the transition region, a systematic experimental investigation on various roughness values of micro-tubes is necessary. However, the science behind these advanced technologies seems to be controversial, especially fueled by the experimental results of the fluid flow and heat transfer at these small scales.

On one hand, researchers have found that the friction factors to be below the classical laminar region theory [3-4]. Meanwhile, some have reported that friction factor correlations for conventional sized tubes to be applicable for mini- and micro-tubes [5-7]. However, many recent experiments on small-sized tubes and channels have observed higher friction factors than the correlations for conventional-sized tubes and channels [8-12], and the cause of this discrepancy was attributed to surface roughness. Ghajar et al. [2] experimentally verified that the wrong selection of pressure sensing diaphragm lead to unrealistic results and frequently the unrealistic results were blamed to be the effect of roughness. Also, Ghajar et al. [2] measured the pressure drop for a horizontal mini- and micro-tubes with various diameters in the transition Reynolds number range under the isothermal condition. Their experimental results indicated the influence of the tube diameter on the friction factor profile and on the transition Reynolds number range. However, the effect of roughness on friction factor profile and transition was still not fully understood. Moreover, only a few studies investigated the effect of heating on friction factor in micro-tubes, especially, in the transition region.

The major objectives of this study are (1) to develop an experimental setup to measure the pressure drop for horizontal micro-tubes under the isothermal and uniform wall heat flux boundary conditions; (2) to accurately measure the pressure drop in different diameter micro-tubes and examine the effect of roughness on the overall pressure drop characteristics, especially, in the transition region; and (3) to examine the effect of heating on the friction factor for micro-tubes.

EXPERIMENTAL SETUP AND DATA REDUCTION

The experimentation for this study was performed using a relatively simple but highly effective apparatus. The apparatus used was designed with the intention of conducting highly accurate heat transfer and pressure drop measurements. The apparatus consists of four major components. These are the fluid delivery system, the flow meter banks, the test section assembly, and the data acquisition system. An overall schematic for the experimental test apparatus is shown in Figure 1. The fluid delivery system consists of a high pressure cylinder filled with ultra high purity nitrogen in combination with a stainless steel pressure vessel. After the working fluid passes through the apparatus, it is collected into a sealed container. The working fluid, distilled water is stored in the stainless steel pressure vessel. As the pressurized nitrogen is fed into the pressure vessel, the working fluid is forced up a stem extending to the bottom of the vessel, out of the pressure vessel, and through the flow meter array and test section.

Flow rate of the water entering the array is further regulated using a metering valve. Two Coriolis flow meters are necessary in order to accommodate different range of flow rates. Both flow meters were factory calibrated. The accuracy of the mass flow rate is within ±0.5%. After passing through the flow meter array, fluid enters the test section assembly. The test section assembly contains the test section as well as the equipment necessary for measurement of inlet and outlet fluid temperature and pressure drop. The test section is placed on a high density polyethylene (HDPE) sheet. Four adjustable bolts and a level were installed on the HDPE board to keep the test section in a horizontal position.

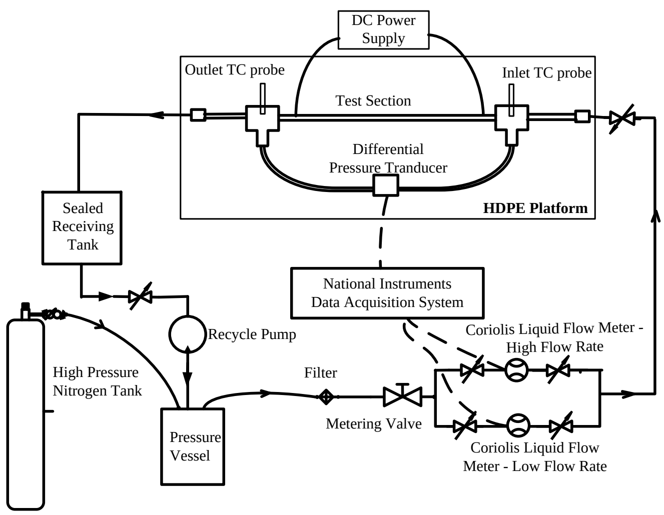

FIGURE 1. SCHEMATIC DIAGRAM OF HEAT TRANSFER AND PRESSURE DROP MEASUREMENT SYSTEM.

In this study, the test sections included the glass tube and the stainless steel tubes with 750μm, 1000μm and 2000μm inner diameters. The 2000μm macro-tube was used for verification of the experimental setup only. For studying the effect of roughness on friction factor, the 750μm and 1000μm micro-tubes with different roughness were used. Different inner surface roughness was made by the acid etching technique.

Different concentrations of acid were used for etching the inner surface of the micro-tubes. 68% nitric acid (HNO3) and 38% hydrochloric acid (HCL) mixed with different volumes of distilled water were injected into the micro-tubes to obtain different surface roughness. Table 1 represents the two methods (Method 1 and Method 2) for getting the different surface roughness of the micro-tubes.

TABLE 1. SURFACE TREATMENT METHODS

Method	Method 1	Method 2
Acid Concentration	10mL 68% HNO3+10mL 38% HCL +100mL distilled water	20mL 68% HNO3+15mL 38% HCL + 50mL distilled water
No. of Injections	10	15
Etching Period after Injections (Hrs.)	4	3
Temperature	Room (20℃)	Room (20℃)

For measuring the inner surface roughness, as seen in Figure 2, a Polytec MSA-500 Stylus 3D Surface Profilometer was used. The value of roughness using different surface roughness treatment methods is shown in Table 2.

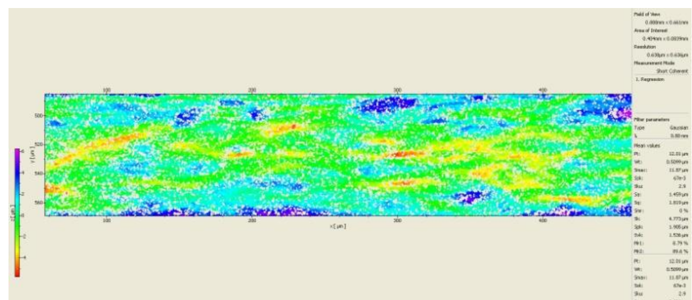

FIGURE 2. ROUGHNESS MEASURED BY THE SURFACE PROFILER.

TABLE 2. SURFACE ROUGHNESS RESULTS

Surface (D=2000μm)	**Ra (μm)**	**ε/D**
Surface 1 (Without Etching)	4.27	0.002135
Surface (D=1000μm)	**Ra (μm)**	**ε/D**
Glass Tube	0	0
Surface 1 (Without Etching)	3.29	0.003298
Surface 2 (Method 1)	3.45	0.003450
Surface 3 (Method 2)	4.32	0.004323
Surface (D=750μm)	**Ra (μm)**	**ε/D**
Surface 1 (Without Etching)	3.38	0.004507
Surface 2 (Method 1)	4.70	0.006267
Surface 3 (Method 2)	4.86	0.006480

Since the stainless steel micro-tubes in this study were purchased from an outside source, data obtained from these tubes is only as accurate as the manufacturer's specifications. In order to ensure that the data recorded was of the highest quality possible, it was deemed necessary to determine the degree of accuracy of the manufacturer's specifications. This was done by using the scanning electron microscope (SEM) for the three different stainless steel tube sizes in order to check the accuracy of the manufacturer's tolerances. Figure 3 shows the SEM measurements for the three stainless tubes. The three stainless steel tubes examined had an inner diameter and tolerance of 2000±32μm, 1000±14μm, and 750±10μm, respectively. The SEM imaging of these three tubes established that the manufacturer's specifications of the tube diameters and tolerances are verifiable and dependable.

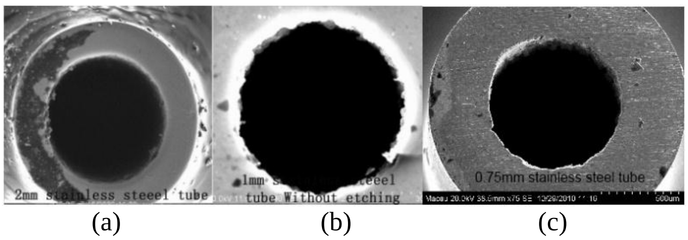

FIGURE 3. SEM MEASUREMENT OF THE STAINLESS STEEL TUBES: (a) 2000μm TUBE; (b) 1000μm TUBE; (c) 750μm TUBE.

As shown in Figure 4, electric copper wires were soldered on to the outside surface of the tubes tested. A DC power supply was used to provide the uniform wall heat flux boundary condition. The voltage was also measured at the soldered position of the tube. For the temperature measurements, the inlet and exit bulk temperatures were measured by means of thermocouple probes (Omega TMQSS-125U-6) placed before and after the test section, respectively. Also, for the heat transfer experiments, self-adhesive thermocouples (Omega SA1XL-T-72) were placed along the test section. All the thermocouples and thermocouple probes were calibrated by a NIST-calibrated thermocouple probe (±0.22℃) and an Omega HCTB-3030 constant temperature circulating bath. Therefore, the temperature sensors were as accurate as ±0.22℃. Figure 4 shows the arrangement of the thermocouples on the test section. The thermocouples were placed at close intervals near the entrance and at greater intervals further downstream. As the diameter of the micro-tube was small, only two surface thermocouples (TC1 and TC2) were located on the periphery of the tube at each station. After installation of the thermocouples, the micro-tube was covered by self-adhesive elastomeric insulating material. From the local peripheral wall temperature measurements at each axial location, the inside wall temperatures and the local heat transfer coefficients were calculated by the method shown in [13]. In these calculations, the axial conduction was assumed negligible (RePr > 2,800 in all cases), but peripheral and radial conduction of heat in the tube wall were included. In addition, the bulk fluid temperature was assumed to increase linearly from the inlet to the outlet. Also, the dimensionless numbers, such as Reynolds, Prandtl, Grashof, and Nusselt were computed by the computer program developed by [13]. The Reynolds number range for this study was around 800 to 13000. Heat balance errors were calculated for all experimental runs by taking a percent difference between two methods of calculating the heat addition. The product of the voltage drop across the test section and the current carried by the tube was the primary method, while the fluid enthalpy rise from inlet to exit was the secondary method. In all cases the heat balance error was less than ±10%.

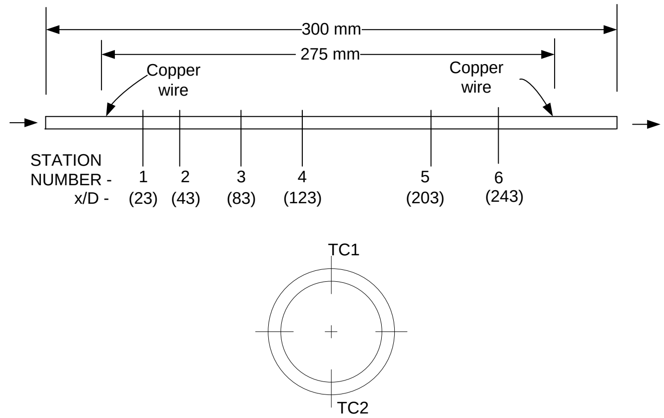

FIGURE 4. ARRANGEMENT OF THE THERMOCOUPLES ON THE TEST SECTION.

For the pressure drop measurements, based on [2], careful attention was paid to the sensitivity of the diaphragms of the pressure transducer. From the manufacturer, the accuracy of the Validyne pressure transducer is given as ±0.25% of the full scale reading of each diaphragm used. In this study, it was confirmed again that different ranging diaphragms would generate different results even in the same Reynolds number range. To ensure the measurement accuracy, a suitable diaphragm was selected based on the Reynolds number range. Calibrations for pressure transducer were performed before each test run. For the calibration purpose, several high accuracy WIKA gauges were used and the pressure reading uncertainty was estimated at ±1.0%.

For data acquisition, a National Instruments SCXI-1000 data collecting system was used. All digital signals from the flow meters, thermocouples, and pressure transducer were acquired and recorded by the Windows-based PC with a self-developed LabView program.

The uncertainty analyses of the overall experimental procedures using the method of [14] showed that there is a maximum ±16% uncertainty for the heat transfer coefficient calculations and a maximum ±5% uncertainty for the friction factor calculations.

RESULTS AND DISCUSSION

To verify the new experimental setup, experiments for 2000μm stainless steel tube were conducted first. Figure 5 shows the comparison of 2,000μm tube heat transfer data with the data of [15] for a 15,800μm stainless steel tube with a square-edged inlet. The square-edged inlet data was used because the inlet of this study was also similar. Since the deviations between the two data sets were below ±10%, the experimental setup and the heat transfer data were confirmed to be reliable. It should be noted that the parallel shift from the classical fully developed value of Nu = 4.364 for the uniform wall heat flux boundary condition in the laminar region is due to the buoyancy effect.

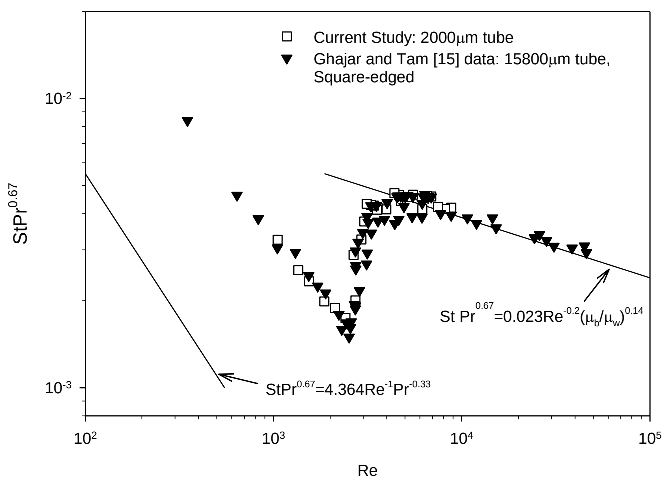

FIGURE 5. COMPARISON OF PRESENT HEAT TRANSFER DATA FOR THE 2000μm DIAMETER STAINLESS STEEL TUBE WITH EXPERIMENTAL DATA [15] AT X/D OF 200.

Based on the careful consideration of the sensitivity of pressure transducer, the measurements of friction factor were also verified by comparing the 2,000μm tube friction factor data with the classical friction factor equations for laminar and turbulent flows. As seen in Figure 6, the 2,000μm tube friction factor data compared very well with the classical fully-developed friction factor equations in the laminar (f = 64/Re) and turbulent (Blasius equation, $f = 0.316/Re^{0.25}$) regions. Figure 6 also shows that the start and end of transition were at Reynolds numbers of around 1,400 and 3,900, respectively. The start of transition Reynolds number of 1,400 was based on the data point just leaving the laminar line, f=64/Re. The end of transition Reynolds number of 3,900, was based on the first data point from the transition region to reach the turbulent line, $f = 0.316/Re^{0.25}$. Owing to the sharp inlet effect, the start of transition is much earlier than the typical transition Reynolds number of 2,300. In Figure 6, the overall friction factor trend over the entire flow regime, especially the transition region, compared well with the experimental data of [2] for a stainless steel tube with a comparable diameter of 2,083μm. Hence, the entire experimental setup for the pressure drop measurements was verified to be reliable.

After the verifications of the experimental setup, the pressure drop measurements under isothermal and heating boundary conditions for the 1,000μm and 750μm micro-tubes were conducted. The results are shown in Figure 7 for friction factor. As seen from the figure, the start and end of transition for friction factor in the 2,000μm macro-tube, 1,000μm and 750μm micro-tubes were established and summarized in Table 3.

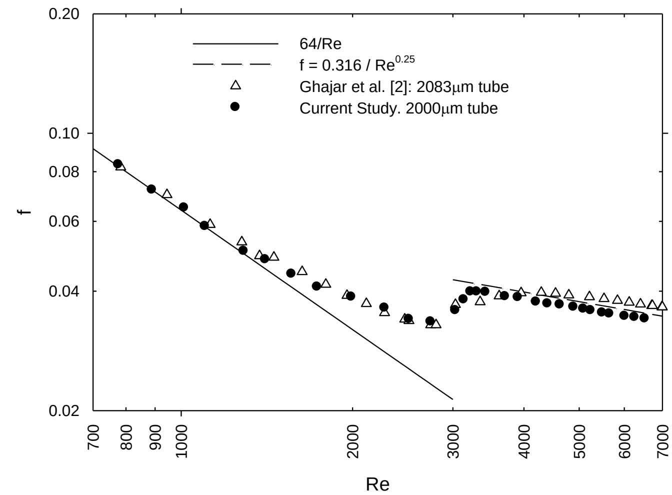

FIGURE 6. COMPARISON OF PRESENT FRICTION FACTOR DATA FOR THE 2000μm DIAMETER STAINLESS STEEL TUBE WITH CLASSICAL EQUATIONS AND EXP. DATA [2].

For the friction factor under isothermal condition, as seen in Figure 7, the laminar and turbulent friction factors for the 1000μm micro-tube exhibited the same behavior as the macro-tube data of the current study and Ghajar's experimental work [2]. Referring to Table 3, the start and end of transition for the 2,000μm macro-tube was nearly the same as the 2,083μm macro-tube of [2]. For the isothermal condition, as shown in Table 3, the lower and upper transition Reynolds numbers of the 1,000μm were 1795 and 3496 which were different from the 2,000μm macro-tube values (Re=1405 and 3704). It can be observed that the transition range of the 1,000μm tube was narrower than that of the 2,000μm tube. Also, the lower and upper transition Reynolds numbers of the 750μm tube were 1816 and 3406 which were different from the 1,000μm micro-tube values. Comparing the 2,000μm, 1,000μm, and 750μm micro-tubes, the 750μm tube has the narrowest transition range. Therefore, it can be observed that the decrease of diameter causes a shorter transition range. This was also consistent with the Ghajar's results [2] for tube diameters ranging from 2083 to 667μm. Results in Table 3 also indicated that for the isothermal case, the decrease in the tube diameter from 2,000μm to 750μm delayed the start of transition.

For friction factor under heating condition, as seen in Figure 8, the laminar and transition friction factor for the micro-tube was shown to be less than the isothermal one. The reduction of friction factor under heating condition was caused by the decrease in the viscosity due to the temperature increase near the tube wall. Also, as seen in Table 3, for the micro-tube, it was observed that heating delayed the start of transition. However, heating did not affect the end of the transition. Moreover, heating did not influence the friction factor in the turbulent region.

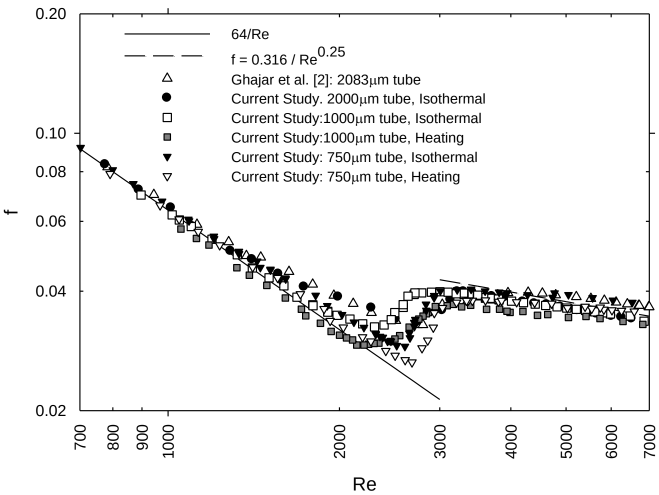

FIGURE 7. FRICTION FACTOR CHARACTERISTICS FOR THE MACRO- AND MICRO-TUBES UNDER ISOTHERMAL AND HEATING BOUNDARY CONDITIONS.

TABLE 3. START AND END OF TRANSITION FOR FRICTION FACTOR OF MACRO- AND MICRO- TUBES (SEE FIG. 7).

Friction Factor				
Tube, Condition	**Re_{start}**	**f**	**Re_{end}**	**f**
Macro-tube, Isothermal Ghajar et al. [2] : 2083μm Stainless Steel Tube	1455	4.87e-2	3954	3.96e-2
Macro-tube, Isothermal Current Study: 2000μm Stainless Steel Tube	1405	4.81e-2	3704	3.88e-2
Micro-tube, Isothermal Current Study: 1000 μm Stainless Steel Tube Without etching	1795	3.70 e-2	3496	3.89 e-2
Micro-tube, Heating Current Study: 1000 μm Stainless Steel Tube Without etching	2144	2.93 e-2	3398	3.69 e-2
Micro-tube, Isothermal Current Study: 750 μm Stainless Steel Tube Without etching	1816	3.90 e-2	3406	4.04 e-2
Micro-tube, Heating Current Study: 750 μm Stainless Steel Tube Without etching	2196	3.06 e-2	3422	3.79 e-2

To establish the effect of different tube roughness, data were first collected from a glass micro-tube with 1000μm diameter and the roughness for the tube was assumed to be zero. The collected data was compared with the 1000μm stainless steel tubes with different inner surface roughnesses and the results are shown in Figure 8. It could be observed that the experimental data of the glass tube in the laminar and turbulent regions perfectly followed the established laminar and turbulent lines and hence the scale effect could not be seen in these regions. However, for the transition region, a narrower transition range was observed. The transition Reynolds number for the glass tube is given in Table 4.

The transition Reynolds numbers for the 1,000μm stainless steel tubes with different roughness values are also documented in Table 4. As illustrated in Figure 8, for the internally rough tubes, no significant deviations were observed in the laminar and turbulent regions. For the transition region, based on Table 4, it can be seen that the lower transition Reynolds number increased as the surface roughness increased and the upper transition Reynolds number decreased as the surface roughness increased. Therefore, it was observed that the range of transition Reynolds number was narrower with the increase of inner surface roughness. To further investigate the effect of roughness and tube diameter, 750μm micro-tubes with different roughness were used to collect data across the complete flow regimes and the results are shown in Figure 9. The transition Reynolds numbers for the 750μm stainless steel tubes with different roughness values are also documented in Table 4. As illustrated in Figure 9, there were no significant deviations observed in the laminar and turbulent regions. However, it was obvious that there were discrepancies among the different roughness curves in the transition region. For the transition region, based on Table 4, it can also be seen that the lower transition Reynolds number increased as the surface roughness increased and the upper transition Reynolds number decreased as the surface roughness increased. Therefore, it was confirmed that, for the 750μm diameter, the range of transition Reynolds number was still narrower with the increase of inner surface roughness.

TABLE 4. START AND END OF TRANSITION FOR FRICTION FACTOR OF THE 1000μm AND 750μm MICRO-TUBES WITH DIFFERENT ROUGHNESSES UNDER ISOTHERMAL CONDITION (SEE FIGS. 8 and 9).

Friction Factor				
Tube, Condition	**Ra(μm)**	**ε/D**	**Re_{start}**	**Re_{end}**
Micro-tube: 1000μm Glass tube Without etching	0	0	1600	4274
Micro-tube: 1000μm, Stainless steel tube Without etching	3.29	0.003298	1795	3496
Micro-tube, Isothermal Current Study: 1000μm Etching (method 1)	3.45	0.003450	2087	3374
Micro-tube, Isothermal Current Study: 1000μm Etching (method 2)	4.32	0.004323	2105	3299
Micro-tube, Isothermal Current Study: 750μm Without etching	3.38	0.004507	1816	3406
Micro-tube, Isothermal Current Study: 750μm Roughness: Etching (method 1)	4.70	0.006267	1902	3201
Micro-tube, Isothermal Current Study: 750μm Etching (method 2)	4.86	0.00648	1989	3203

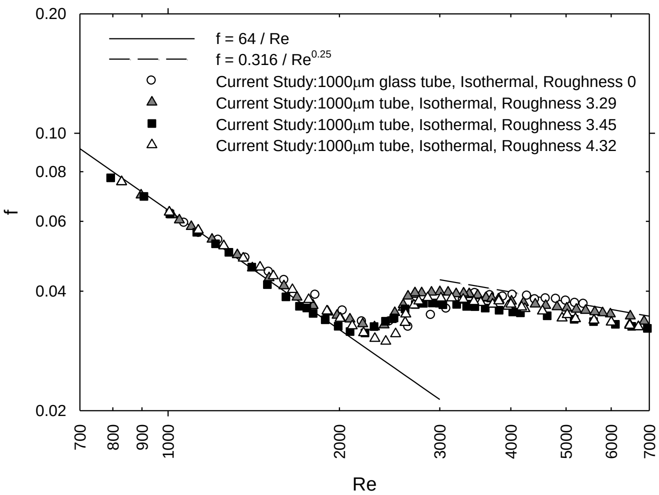

FIGURE 8. FRICTION FACTOR CHARACTERISTICS FOR THE 1000µm MICRO-TUBES WITH DIFFERENT ROUGHNESSES UNDER ISOTHERMAL BOUNDARY CONDITIONS.

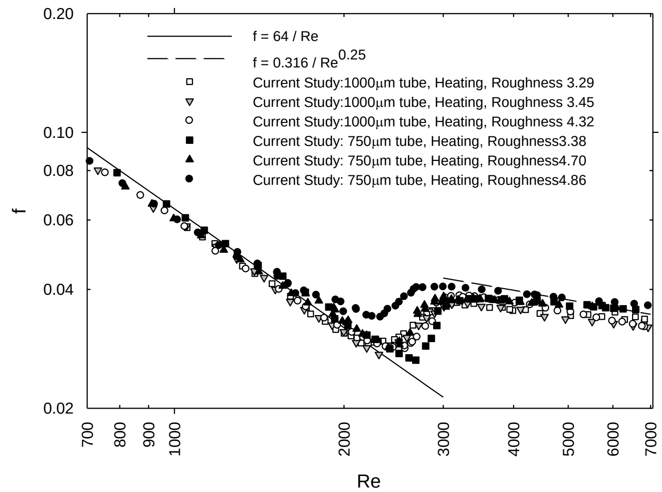

FIGURE 10. FRICTION FACTOR CHARACTERISTICS FOR THE 1000µm AND 750µm MICRO-TUBES WITH DIFFERENT ROUGHNESSES UNDER HEATING BOUNDARY CONDITION.

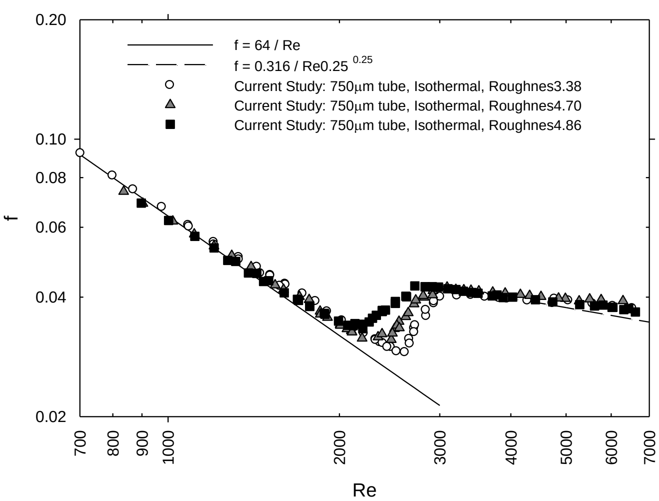

FIGURE 9. FRICTION FACTOR CHARACTERISTICS FOR THE 750µm MICRO-TUBES WITH DIFFERENT ROUGHNESSES UNDER ISOTHERMAL BOUNDARY CONDITION.

TABLE 5. START AND END OF TRANSITION FOR FRICTION FACTOR OF THE 1000µm AND 750µm MICRO-TUBES WITH DIFFERENT ROUGHNESSES UNDER HEATING CONDITION (SEE FIG. 10).

Friction Factor				
Tube, Condition	**Ra(µm)**	**ε/D**	**Re_{start}**	**Re_{end}**
Micro-tube, Heating Current Study: 1000µm Without etching	3.29	0.003298	2144	3398
Micro-tube, Heating Current Study: 1000µm Etching (method 1)	3.45	0.003450	2306	3313
Micro-tube, Heating Current Study: 1000µm Etching (method 2)	4.32	0.004323	2373	3338
Micro-tube, Heating Current Study: 750µm Without etching	3.38	0.004507	2196.	3422
Micro-tube, Heating Current Study: 750µm Etching (method 1)	4.70	0.006267	2296	3186
Micro-tube, Heating Current Study: 750µm Etching (method 2)	4.86	0.00648	2100	2999

Figure 10 shows the friction factor characteristics for the 1000µm and 750µm micro-tubes with different roughness under heating condition. Table 5 shows the start and end of transition values of the 1000µm and 750µm tubes with different roughness under the heating condition. Comparing with the isothermal results of Table 4, it could be concluded that the general effect of heating is to delay the start of transition. Under the heating condition, as shown in Table 5, it could also be concluded that the range of transition Reynolds number was narrower with the increase of inner surface roughness regardless of the tube diameter.

CONCLUDING REMARKS

In this study, an experimental setup was designed and verified for the measurements of pressure drop (friction factor) and heat transfer in horizontal micro- and macro- tubes under uniform wall heat flux boundary condition in all flow regimes (laminar-transition-turbulent). To verify the new experimental setup, experiments for 2000µm tube were conducted first. Then, the pressure drop measurements under isothermal and heating boundary conditions for the 1,000µm and 750µm micro-tubes with different roughnesses were also conducted.

Comparing the results for the different diameter tubes (from 2000µm to 750µm), it could be concluded that, for friction factor under isothermal condition, the decrease of tube diameter induced a narrower transition range and delayed the start of transition. The narrower transition range induced by the decrease of diameter was also consistent with the Ghajar's results [2] for tube diameters ranging from 2083 to 667μm.

For friction factor under heating condition, it was concluded that heating for micro-tube reduced the laminar and transition friction factor and delayed the start of transition. However, heating did not affect the end of transition and the turbulent friction factor.

Finally, comparing the different roughnesses of the 1000μm and 750μm micro-tubes under the isothermal and heating conditions, it was concluded that the range of transition Reynolds number was narrower with the increase of inner surface roughness.

ACKNOWLEDGMENTS

This research is supported by the Fundo para o Desenvolvimento das Ciencias e da Tecnologia under project no. 033/2008/A2 and the Institute for the Development and Quality, Macau.

REFERENCES

[1] Krishnamoorthy, C., Rao, R. P., and Ghajar, A. J., 2007, "Single-Phase Heat Transfer in Micro-Tubes: A Critical Review," *Proceedings of the 2007 ASME-JSME Thermal Engineering Summer Heat Transfer Conference*, Vancouver, British Columbia, Canada, July 8-12.

[2] Ghajar, A. J., Tang, C. C., Cook, W. L., 2010, "Experimental Investigation of Friction Factor in the Transition Region for Water Flow in Mini-tubes and Micro-tubes," *Heat Transfer Engineering*, **31**(8), pp. 646-657.

[3] Choi, S. B., Barron, R. F., and Warrington, R. O., 1991, "Fluid Flow and Heat Transfer in Micro-tubes," *Proceedings of Winter Annual Meeting of the ASME Dynamic Systems and Control Division*, Atlanta, GA, Vol. 32, pp. 123-134.

[4] Yu, D., Warrington, R., Barron, R., and Ameel, T., 1995, "Experimental and Theoretical Investigation of Fluid Flow and Heat Transfer in Microtubes," *Proceedings of the 1995 ASME/JSME Thermal Engineering Joint Conference*, Maui, HI, Vol. 1, pp. 523−530.

[5] Mala, G. M., Li, D. Q., 1999, "Flow characteristics of water in micro-tubes," *International Journal of Heat and Fluid Flow*, **20**(2), pp. 142-148.

[6] Kandlikar, S. G., Joshi, S., and Tian, S., 2003, "Effect of Surface Roughness on Heat Transfer and Fluid Flow Characteristics at Low Reynolds Numbers in Small Diameter Tubes." *Heat Transfer Engineering*, **24**(3), pp. 4-16.

[7] Li, Z. X., Du, D. X., and Guo, Z. Y., 2003, "Experimental Study on Flow Characteristics of Liquid in Circular Microtubes," *Nanoscale and Microscale Thermophysical Engineering*, **7**(3), pp. 253−265.

[8] Zhao, Y., and Liu, Z., 2006, "Experimental studies on Flow Visualization and Heat Transfer Characteristics in Micro-tubes," *Proceeding of the 13th International Heat Transfer Conference*, Sydney, Australia, MIC-12.

[9] Hwang, Y. W. and Kim, M. S., 2006, "The Pressure Drop in Microtubes and the Correlation Development," *International Journal of Heat and Mass Transfer*, **49**(11−12), pp. 1804−1812.

[10] Rands, C., Webb, B. W. and Maynes, D., 2006, "Characterization of transition to turbulence in microchannels," *International Journal of Heat and Mass Transfer*, **49**(17-18), pp. 2924-2930.

[11] Celeta, G.P., Cumo, M., McPhail, S., Zummo, G., 2006, "Characterization of fluid dynamic behavior and channel wall effects in micro-tube," *International Journal of Heat and Fluid Flow*, **27**(1), pp. 135-14

[12] Tang, G. H., Li, Z., He, Y. L., and Tao, W. Q., 2007, "Experimental Study of Compressibility, Roughness and Rarefaction Influences on Microchannel Flow," *International Journal of Heat and Mass Transfer*, **50**(11−12), pp. 2282−2295.

[13] Ghajar, A. J. and Kim, J., 2006, "Calculation of local inside-wall convective heat transfer parameters from measurements of the local outside-wall temperatures along an electrically heated circular tube," *Heat Transfer Calculations, edited by Myer Kutz, McGraw-Hill, New York*, NY, pp. 23.3-23.27.

[14] Kline, S. J., and McClintock, F. A., 1953, "Describing Uncertainties in Single Sample Experiments," Mech. Eng., **75**, pp. 3-8.

[15] Ghajar, A. J. and Tam, L. M., 1994, "Heat transfer measurements and correlations in the transition region for a circular tube with three different inlet configurations", *Experimental Thermal and Fluid Science*, **8**(1), pp. 79-90.